

Properties of Titanium Oxynitride Prepared by RF Plasma

Fayez M. El-Hossary, Niemat Z. Negm, Ahmed M. Abd El-Rahman, Mohamed Raaif, Alzahraa A. Abd Elmula

Physics Department, Faculty of Science, Sohag University, Sohag, Egypt
Email: mraaif@daad-alumni.de

Received 25 October 2014; revised 25 November 2014; accepted 9 December 2014

Copyright © 2015 by authors and Scientific Research Publishing Inc.
This work is licensed under the Creative Commons Attribution International License (CC BY).
<http://creativecommons.org/licenses/by/4.0/>



Open Access

Abstract

Titanium oxynitrides combine the properties of metallic oxides and nitrides. In this presentation, titanium was oxynitrided using inductively coupled RF plasma in a gas mixture containing 80% N₂ and 20% O₂. The effect of plasma-processing power from 350 up to 550 W on microstructure, mechanical, tribological, wettability and electrochemical properties of the oxynitrided titanium was examined using different characterizations and testing techniques. The results demonstrated the formation of TiO, TiO₂ rutile phase, TiN_xO_y and Ti₂N as a result of plasma oxynitriding. The microhardness of the oxynitrided layers increases up to 766 HV_{0.1} as the plasma-processing power increases up to 550 W. The wear and corrosion resistance are improved for oxynitrided titanium in comparison with untreated samples. Moreover, the friction coefficient decreases from nearly 0.75 for the pure titanium to nearly 0.3 for oxynitrided titanium. The obtained data show an increase of surface energy and wettability of titanium oxynitride as the plasma power increases. The formation of hard oxide and oxynitride phases and the transformation of TiO₂ from anatase to rutile structure at relatively high temperature are the main reasons for the good physical and electrochemical properties of titanium oxynitride.

Keywords

Plasma Oxynitriding, Titanium, Corrosion, Wear, Hardness, Surface Energy and Wettability

1. Introduction

Titanium and titanium alloys have many attractive properties including relatively high specific strength and modulus, good corrosion resistance and biocompatibility. Therefore, they are widely used in many branches of industries [1]-[4]. However, titanium and titanium alloys have found modest use in general engineering applications, mainly because of their meager tribological properties [5]. In order to improve such properties, one prom-

ising way of titanium surface engineering is through the formation of titanium oxynitrides (TiN_xO_y) in the top surface. Titanium oxynitrides have a great importance in many sectors of applications because of their enormous physical and chemical properties that exceed the properties of titanium nitrides or titanium oxides [6]. In particular, titanium oxynitrides are widely used in medicine and in chemical industries because of excellent combination of chemical and mechanical properties [7] [8]. Nowadays, there is a growing interest in the methods of thermo-chemical treatment connected with diffusion saturation of material surface by different elements. The processes such as oxidizing [9], carburizing [10] and nitriding [11] can increase the wear and corrosion resistance, decrease the coefficient of friction and easily harden the surface of the material. The present work is planned with the aim of enhancing the physical and electrochemical properties of titanium by modifying the surface microstructure through oxynitriding using RF plasma treatment. The properties and the characteristics of the processed samples are evaluated using X-ray diffraction (XRD), optical microscopy, microhardness tester, surface profile, oscillating ball-on-disk tribometer, contact angle analyzer and Gill AC instrument for corrosion measurements.

2. Experimental

2.1. Sample Treatment

Pure titanium substrates with dimensions of $10 \text{ mm} \times 10 \text{ mm} \times 1 \text{ mm}$ were used in this study. The samples were polished and ultrasonically cleaned in acetone bath for 15 min before inserting them into the plasma reactor tube. The samples were oxynitrided using radio frequency (RF) plasma inductively coupled operated in continuous mode. Details of the system can be found somewhere else [12] [13]. In brief, the RF plasma system is comprised of a quartz reactor tube with length of 500 mm and a diameter of 41.5 mm and it was evacuated to a base pressure of 1.0×10^{-2} mbar by a two-stage rotary pump. The titanium samples were centered in the RF coil on a supported titanium bar of 2.9 cm length and 1 cm diameter which is fixed on a water-cooled copper sample holder. The oxynitrided process was performed using a gas mixture containing 80% nitrogen and 20% oxygen, and the gas flow rates were adjusted to establish a total gas pressure of 7.5×10^{-2} mbar, as measured by a capacitance manometer. The induction copper coil, energized by an RF power generator model HFS 2500 D at 13.65 MHz via a tunable matching network, generated the discharge. The samples were treated at a different plasma-processing power from 350 W to 550 W with a step of 50 W and for processing time of 10 minutes. It is important to state that, this treatment process was performed without using any external source of heating. The sample temperature was measured during the RF plasma process by a chromel-alumel thermocouple, which is placed closed to the surface of the sample. The sample temperature is varied from 905°C - 1030°C as the plasma power varied from 350 - 550 W. After the oxynitriding process, the samples were allowed to cool slowly in the evacuated reactor plasma tube.

2.2. Samples Characterization

XRD analyses of the investigated samples were performed using a Philips X-ray diffractometer PW1710 with $\text{Co K}\alpha$ radiation of $\lambda = 1.78896 \text{ \AA}$ to characterize the crystallographic configuration of the samples. The patterns of the X-ray diffraction analysis were run in a normal $\theta - 2\theta$ scan between 30° and 95° with step intervals of 0.02° and scan rate of $2^\circ/\text{min}$. Vickers microhardness measurements were carried out for the oxynitrided surfaces using a Leitz Durimet microhardness tester with a contact load of 100 g. The microhardness measurements were performed according to ASTM E384-11 standard test method at temperature of $25^\circ\text{C} \pm 3^\circ\text{C}$ [14]. The microhardness tester has been accredited according to ISO/IEC 17025:2005 requirements.

The surface roughness was measured using a Form Talysurf 50 which has been accredited according to ISO/IEC 17025:2005 requirements. The cross-section morphology of the treated titanium was investigated using Olympus BX51 optical microscope. The wear measurements were performed at room temperature in air atmosphere with humidity of 35% - 40% using an oscillating ball-on-disk type tribometer wear tester without lubrication. The wear measurements were performed according to ASTM G 133-10 standard test method (linearly reciprocating ball-on flat sliding wear). The 6 mm ball of alumina (Al_2O_3) moves at a mean sliding speed of 2 mm/s with a normal load of 2 N has been used. During the wear measurements, the friction coefficient was continuously measured by using a force sensor. The oscillating ball-on-disk type tribometer wear tester is accredited according to ISO/IEC 17025:2005 requirements. The water contact angle measurement, at room temperature,

was used to determine hydrophilicity of the treated surface using a Phoenix 300 (Contact Angle Analyzer manufactured by S.E.O Co. Ltd.). The Phoenix 300 utilized a precision camera and an advanced PC technology to capture the static droplet image and to calculate the contact angle by Sessile Drop method.

The electrochemical experiments were carried out using Gill AC instrument. The untreated and treated samples were tested in Ringer's solution at $25^{\circ}\text{C} \pm 3^{\circ}\text{C}$. The exposed area to corrosive solution was fixed at 0.36 cm^2 for all samples. The potentiodynamic polarization test was performed using three-electrodes; silver-silver chloride saturated electrode as a reference electrode, platinum as a counter electrode and the investigated sample as a working electrode. The potential-current corrosion curve is recorded and plotted with potential scan rate of 1 mV/s using Gill AC instrument and ACM program version 5.

3. Results and Discussion

3.1. X-Ray Analysis

The XRD patterns of the oxynitrided titanium at different plasma-processing powers using a gas mixture containing 80% N_2 and 20% O_2 are presented in **Figure 1**. The patterns indicate that the main phases observed after oxynitrided of titanium are TiO , TiO_2 rutile, TiN_xO_y and Ti_2N , which form the compound layer in the top of the entire titanium surface. The X-ray diffractogram reveals the formation of minor phase of TiO which is characterized by (101), (002), (200) reflections. Moreover, the TiO_2 rutile phase has been detected too with no evidence for the formation of TiO_2 anatase phase. The TiO_2 rutile phase is characterized by (110), (101), (200), (111), (220), (310), (112) reflections. The rutile phase has a preferred orientation in the (110) direction whereas the intensity increases as the plasma-processing power increases. The formation of rutile phase is judged from the fact that, the treatment of titanium is performed at high temperature in which most of anatase phase transformed to rutile phase. The rutile structure is more compact than anatase one and it has higher hardness and wear resistance. Chappe *et al.* [15] achieved a large amount of rutile phase at 673 K. Qiong Weng *et al.* [16] demonstrated that, the TiO_2 rutile phase is thermodynamically stable phase and it has perfect crystalline structure with high electron density and low cavity density.

The peaks of oxynitrided titanium phase have been observed at 2θ equal 41.2° and 49.5° which have reflections of (111) and (200). Since the stoichiometry of TiNO is not determined, it is generally termed as TiN_xO_y . The formation mechanism of TiNO can be enlightened by the higher reactivity of oxygen with metal surface in which metal-oxygen bonds over metal-nitrogen bonds can be formed. These phases are accomplished from the hasty substitutions of nitrogen vacancies by oxygen atoms [17]. The nitrogen in TiN is swapped by oxygen and

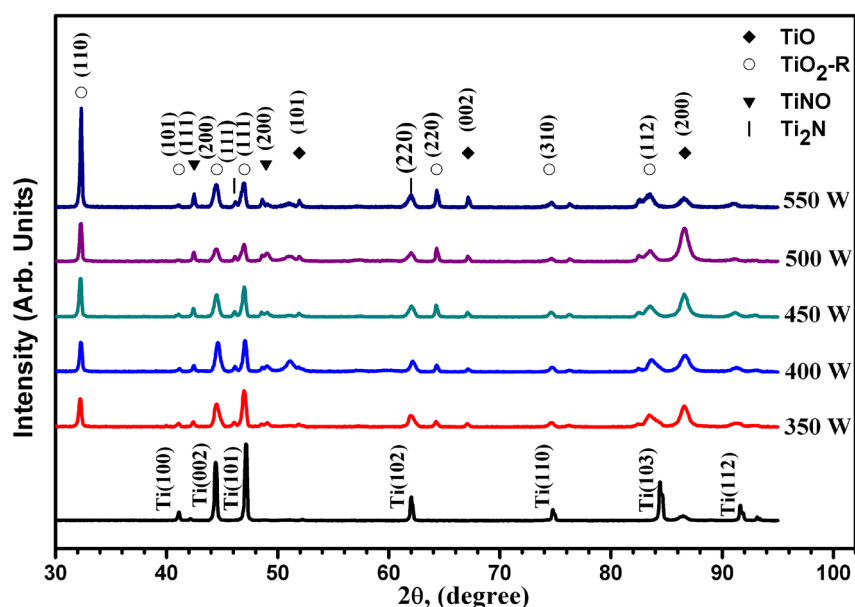


Figure 1. The XRD patterns of the oxynitrided titanium at different plasma-processing powers.

forms TiN-TiO solid solution, *i.e.* titanium oxynitride. According to [18] [19], the substitution of nitrogen by oxygen in TiN_xO_y phase leads to local lattice constant reduction. The decrease in the lattice dimensions constructs a more compact of TiN_xO_y phase which in turn improve the mechanical and tribological properties of the matrix.

Other peaks are presented at 2θ equal 46.08° and 62.1° and have (111) and (220) reflections, respectively. These peaks fit well with Ti_2N phase. It is worth mentioned that enhanced the substrate temperature leads to a better crystallization of the oxide phases [20]. The formation of TiO_2 rutile phase, TiN_xO_y and Ti_2N hard phases are the reason for the superior mechanical and tribological properties of titanium oxynitride.

According to Williamson and Hall [21] based on the work of Scherrer [22] and Wilson [23], the strain and the grain size of the TiN_xO_y can be determined from the X-ray diffraction patterns. Williamson and Hall developed a method known as Williamson Hall Plot

$$\beta = \frac{K\lambda}{D_\beta \cos\theta} + 4 \cdot \varepsilon \tan\theta$$

where β is the integral peak width, K is the Scherrer factor close to unity, D_β is the grain size, and ε is the maximum strain in the lattice parallel to the reflection planes. Plotting $\frac{\beta \cos\theta}{\lambda}$ versus $\frac{\sin\theta}{\lambda}$ results a linear fit in

which the slope and the intercept can be determined. **Figure 2** shows the relationship between $\frac{\beta \cos\theta}{\lambda}$ and $\frac{\sin\theta}{\lambda}$ for the sample that was oxynitrided at a plasma-processing power of 550 W as an example for the Williamson Hall Plot. From the linear relationship shown in the figure, the slope of the line which represents 4ε and the intercept of the line which represents $\frac{\beta \cos\theta}{\lambda}$ or $1/D_\beta$ can be calculated. **Figure 3** represents the grain size

of the oxynitrided titanium as a function of plasma-processing power. One can observe from the figure that, the grain size increases from nearly 50 nm for the sample that was oxynitrided at plasma power of 350 W to approximately 110 nm for the sample that was oxynitrided at plasma-processing power of 550 W.

3.2. Microhardness

Figure 4 shows the microhardness variation of the untreated and oxynitrided titanium as a function of plas-

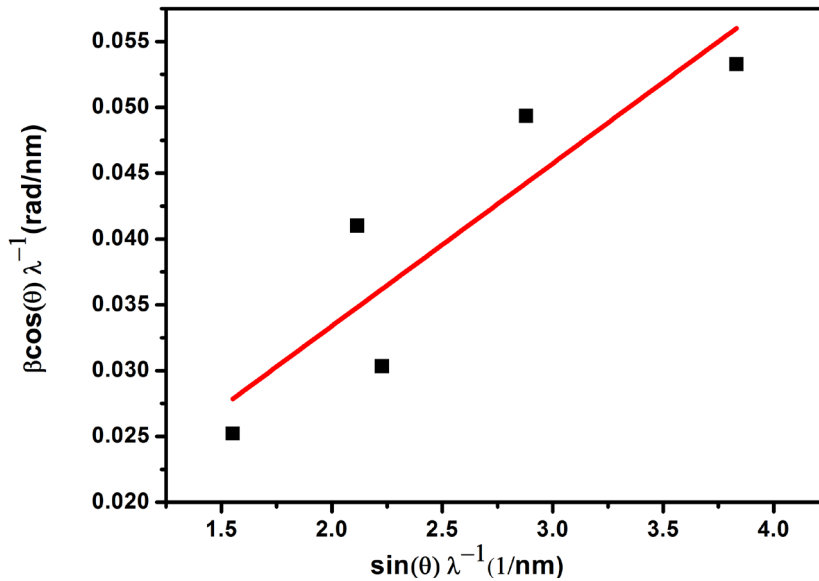


Figure 2. Williamson Hall Plot for the sample that was oxynitrided at plasma processing power of 550 W.

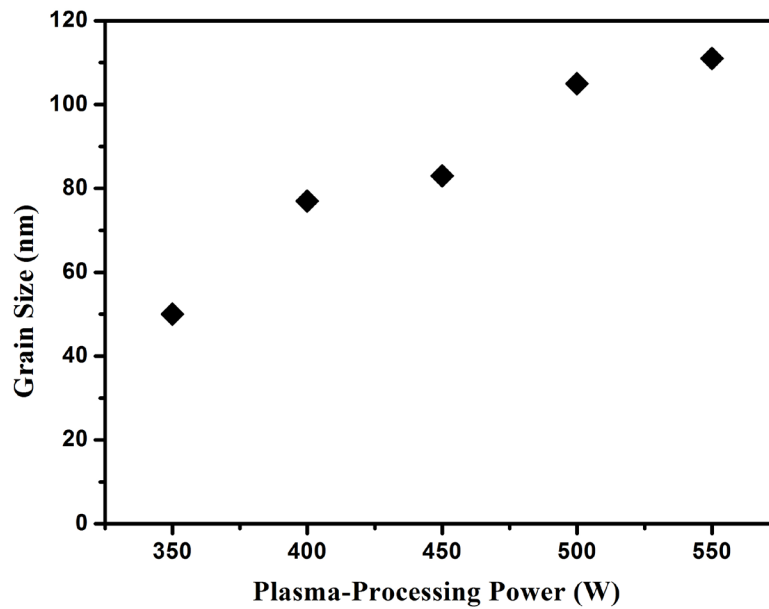


Figure 3. Grain size of the oxynitrided titanium as a function of plasma-processing power.

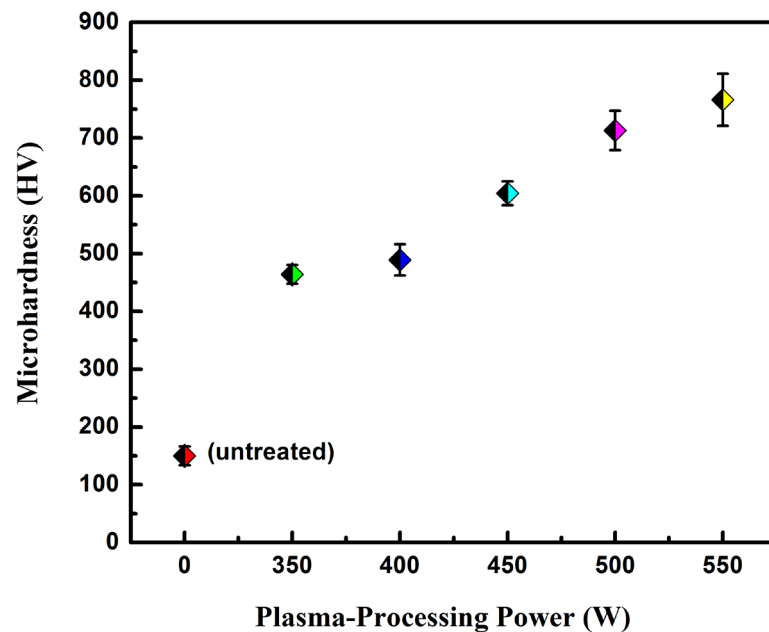


Figure 4. Surface microhardness of the oxynitrided titanium versus plasma-processing power.

ma-processing power. One can notice from the figure that, the microhardness increases up to 766 HV_{0.1} as the plasma-processing power increases up to 550 W. This value represents 5-folds increase in microhardness in comparison with the untreated titanium sample. The increase in microhardness is ascribed to the formation of, TiO₂ rutile, TiN_xO_y, Ti₂N hard phases. The supplementary increase in the microhardness at higher plasma-processing power could be ascribed to the high intensity of TiO₂ rutile phase and to the transformation of TiO₂ from anatase to rutile structure at relatively high temperature. The rutile structure is more densely packed (4.250 g/cm³) than anatase structure (3.899 g/cm³) [24]. For this reason the rutile structure is more compact, harder and has higher wear resistance than anatase structure. Abboud [25] and Qiong Weng *et al.* [16] have achieved a sig-

nificant improvement in the surface hardness due to the presence of TiO_2 .

3.3. Layer Thickness

Figure 5 signifies the oxynitrided layer thickness as a function of plasma-processing power. One can find out from the figure that, the layer thickness increases as the plasma-processing power increases. The layer thickness increases from nearly $4 \mu\text{m}$ for the sample that was oxynitrided at a processing power of 350 W to approximately $8 \mu\text{m}$ for the sample that was oxynitrided at a processing power of 550 W. The lower value of the layer thickness with respect to nitriding process could be ascribed to the lower enthalpy of oxides (*i.e.* low diffusion coefficient) than nitrides. Thus the oxygen diffusion inside the metal cannot take place on a long scale and in turn oxides are precipitated in the near surface region [26].

3.4. Roughness Measurements

Figure 6 represents the root mean square (RMS) and average roughness (Ra) for the untreated and oxynitrided titanium as a function of plasma-processing power. One can observe from the figure that the RMS and Ra of the oxynitrided titanium are greater than that of the untreated one. Moreover, the RMS and Ra for the oxynitrided titanium increase as the plasma-processing power increases. The increase in surface roughness of the oxynitrided samples in comparison with the untreated titanium could be ascribed to the change in surface topography due to the formation of oxynitrided layer in the top titanium surface, which in turn increases the surface irregularities [27]. Furthermore, the continues increase in surface roughness of the oxynitrided titanium as the plasma-processing power increases can be attributed to the gradual increase in the surface temperature as the plasma-processing power increases. It is well known that, the production of energetic plasma species increases the surface temperature. This will lead to the increase in chemical and physical reactions between the plasma species and the plasma immersed material and in turn growing the surface roughness.

3.5. Wear and Friction Measurements

The wear behavior of the untreated and oxynitrided titanium was evaluated using oscillating ball-on-disk type tribometer. **Figure 7** and **Figure 8** show the optical micrographs and wear track profiles of the untreated and oxynitrided titanium at different plasma power respectively. One can monitor from the two figures that, the wear track dimensions of the untreated titanium is greater than that of the oxynitrided titanium. Further, the wear track dimensions for the oxynitrided titanium decrease with increasing the plasma-processing power. **Figure 9** represents the wear rate of the investigated titanium samples as a function of plasma-processing power, where

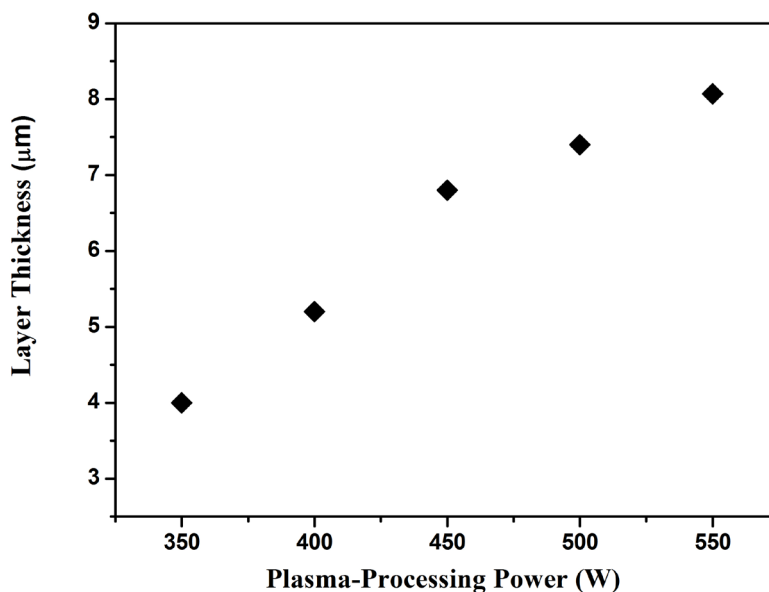


Figure 5. Oxynitrided layer thickness as a function of plasma-processing power.

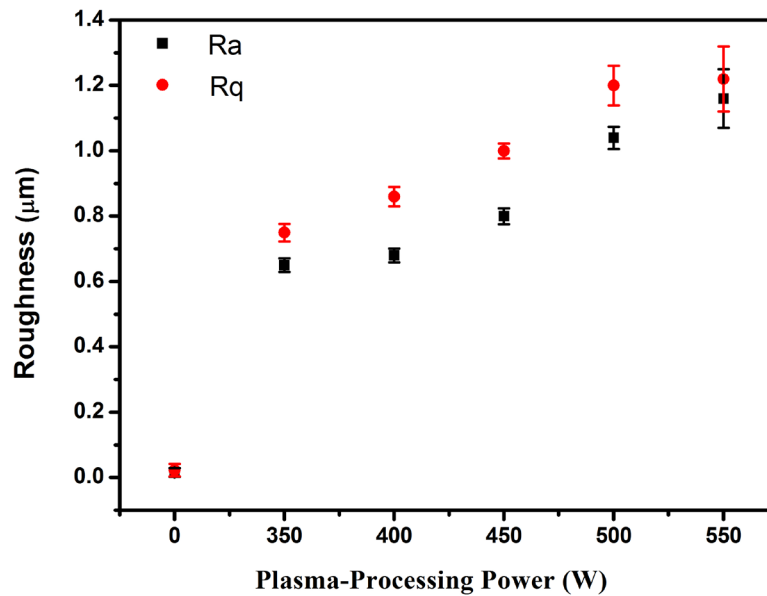


Figure 6. RMS and Ra for the untreated and oxynitrided titanium as a function of plasma-processing power.

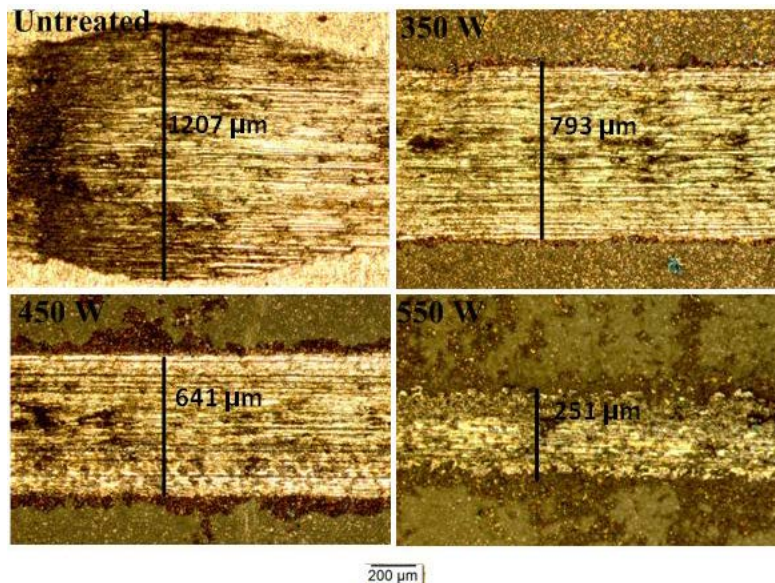


Figure 7. Optical micrograph of wear tracks for the untreated and oxynitrided titanium at different plasma processing-power.

the wear rate is calculated as the *wear area* \times *track length* / *total sliding distance*. One can detect from the figure that, the wear rate decreases as the plasma-processing power increases. The decrease in the wear rate is ascribed to the surface strengthening resulting from the formation of hard phases of TiO_2 rutile, TiN_xO_y and Ti_2N precipitates in the near-surface region of Ti. The high hardness of these phases combines with high ductility of the base material imparts significant strength to the surface and consequently improvement in the wear resistance. Stratton *et al.* [28] ascribed the enhancement in titanium wear resistance to the presence of rutile TiO_2 in the compound layer. He reported that, after heat treatment of Ti-6Al-4V in argon/oxygen atmosphere, rutile surface oxide (TiO_2) is produced and an optimum wear characteristic to the titanium alloy surface is obtained. These results are consistent with the microhardness values, where the hardness increases with the increase in plasma-processing power. The treated samples at higher plasma power show less susceptible to plastic deformation

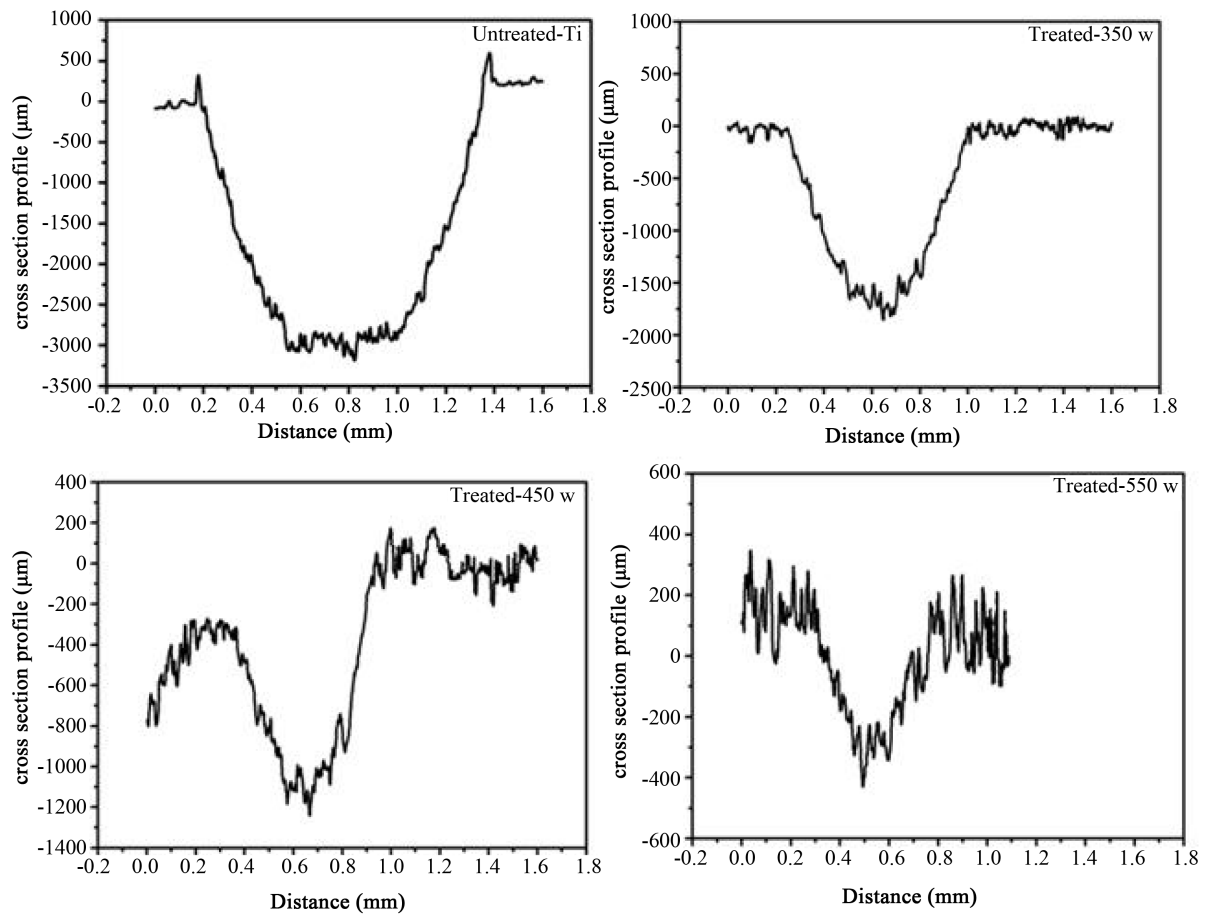


Figure 8. Cross-profile of the central region of wear tracks for the untreated and oxynitrided titanium at different plasma-processing power.

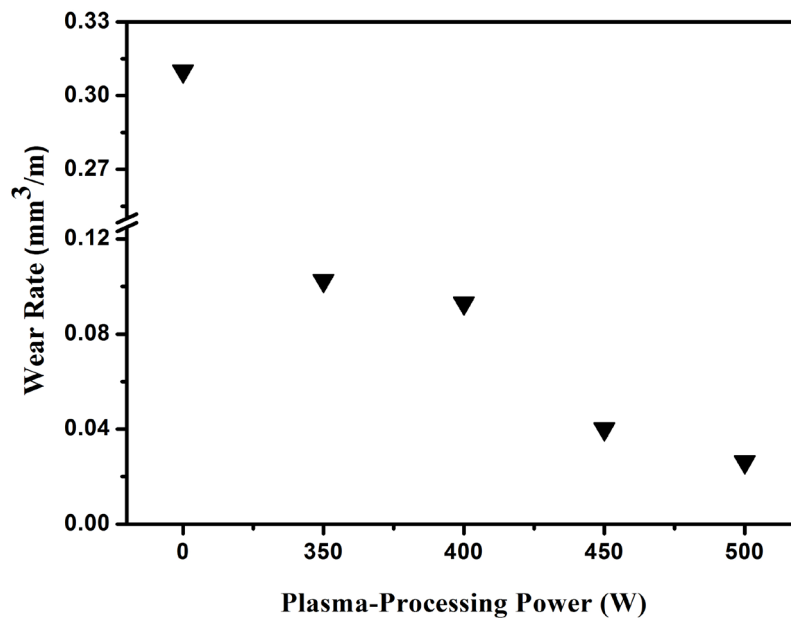


Figure 9. The wear rate of the investigated titanium samples as a function of plasma-processing power.

under the applied normal loads.

Through the wear measurements, the recording of the friction coefficient was continuously measured using a force sensor. **Figure 10** characterizes the friction coefficient of the untreated and plasma oxynitrided titanium at different plasma-processing powers. From this figure, the friction coefficient decreases from nearly 0.75 for the untreated titanium to nearly 0.3 for the oxynitrided titanium. Introducing a large volume fraction of nitrogen and oxygen species, change the chemistry of the surface that accompanied by a decrease in the friction coefficient. Furthermore, the tribo-oxide film of TiO_2 formed during sliding wear in addition to the TiO_2 rutile phase formed during the plasma treatment is considered as another contributing factor in decreasing the friction coefficient. **Figure 11** represents the relation between the friction coefficient and the sliding distance for the untreated and

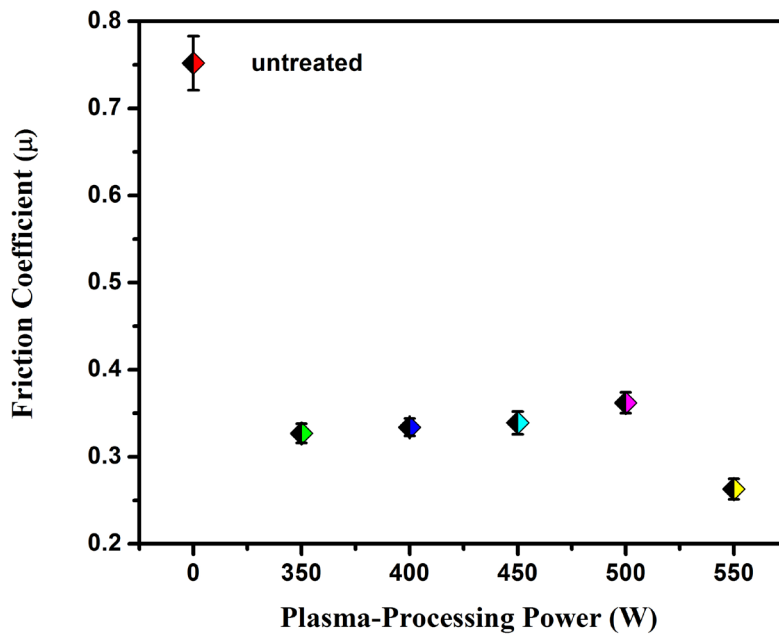


Figure 10. Friction coefficient of the untreated and plasma oxynitrided titanium samples at different plasma-processing powers.

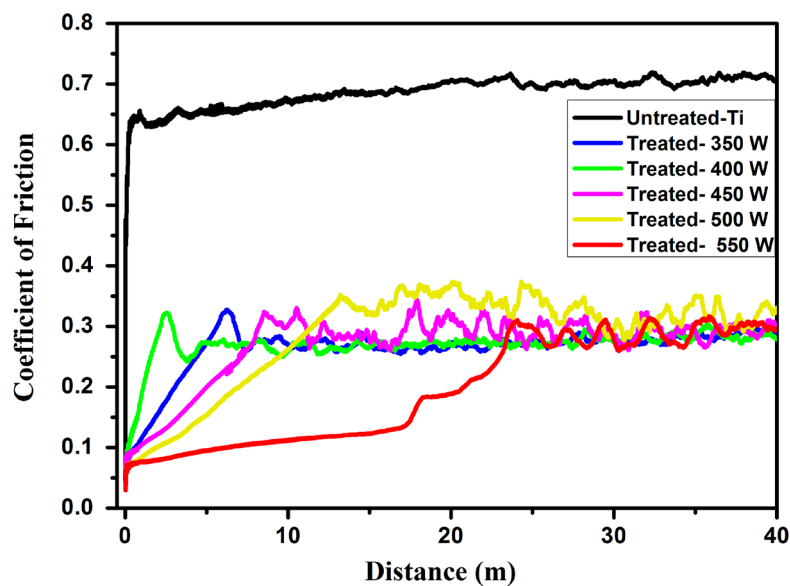


Figure 11. The relation between the friction coefficient and the sliding distance for the untreated and oxynitrided titanium.

oxynitrided titanium. This figure shows no brittle failure in the oxynitrided layer after 2000 tracks and the friction coefficient increases as the sliding distance increases. This behavior could be related to the decrease of the concentration of nitrogen and oxygen as the depth increases. Furthermore, the decrease in the friction coefficient for the untreated titanium sample at low sliding distance is due to the existence of native oxide layer on the top of the metal surface. At the end of the native oxide layer, a breakthrough in the friction coefficient will occurred and it accompanied by the formation of fragments on the wear track and in turn increases the friction coefficient [29]. Tapash *et al.* [30] demonstrated that, the native oxide layer formed on the surface of titanium or its alloys provides a useful low-friction surface; when this oxide layer is removed, rapid adhesive wear occurs against many counter-face materials. To combat this oxide removal, Ti surface can be hardened by changing the surface chemical composition using plasma nitriding or oxynitriding. The increase in surface hardness accompanied with high ductility of the base matrix allows the material to resist the plastic deformation during the wear test.

3.6. Corrosion Performance

The typical potentiodynamic polarization curves for the untreated and oxynitrided titanium in Ringer’s solution at room temperature are presented in **Figure 12**. Additionally, the average values of the corrosion potential (E_{corr}) and the corrosion current density (I_{corr}) are calculated from the polarization curves for all tested samples and listed in **Table 1**. The results show that, the untreated titanium has highest corrosion current density in comparison

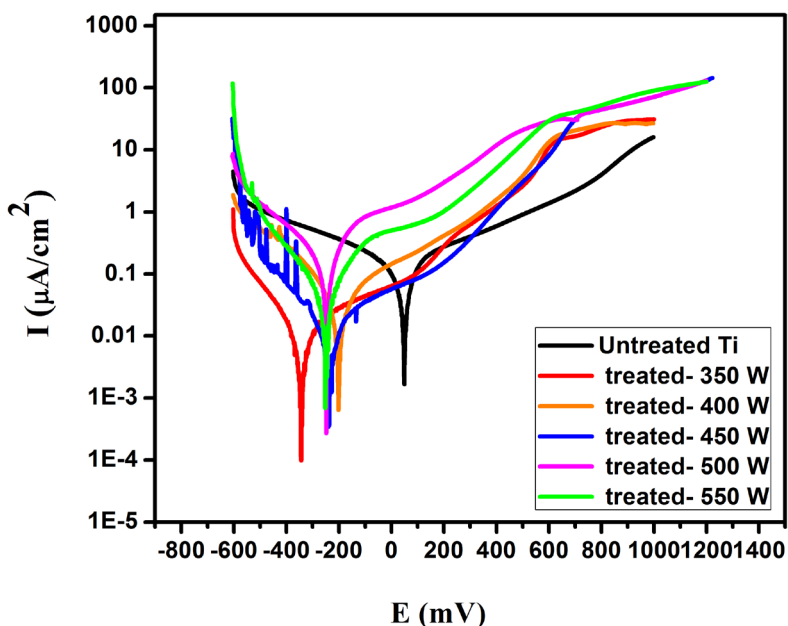


Figure 12. Tafel curves for the untreated and oxynitrided titanium in Ringer’s solution at room temperature.

Table 1. Corrosion data for the untreated and oxynitrided titanium sample in Ringer’s solution.

Plasma-processing power (w)	I_{corr} ($\times 10^{-5}$ mA/cm ²)	E_{corr} (mv)	Corrosion rate ($\times 10^{-5}$ mm/year)
Untreated-Ti	13	50	22.6
350	0.229	-344	1.62
400	3.25	-203	5.66
450	1.02	-239	1.78
500	8.3	-254	14.4
550	4.3	-251	7.4

with the untreated titanium in the cathodic part. On the other hand, the corrosion current density is nearly the same for all tested samples in the anodic zone at corrosion potential lower than 300 mV. For corrosion potential greater than 300 mV in the anodic zone, the oxynitrided titanium has corrosion current greater than the untreated titanium. This behavior is ascribed to the increase in surface roughness due to the plasma oxynitriding process [31]. One can notice from the figure that, the oxynitrided titanium has the ability to form stable passive layer after corrosion potential of 600 mV, and no passivation has been observed for the untreated titanium. As demonstrated in **Table 1**, the corrosion resistance of the untreated titanium is lower than that of the oxynitrided titanium. This performance is attributed to the formation of anti-corrosive layer formed from TiO_2 rutile, TiN_xO_y and Ti_2N precipitates in the near-surface region of Ti. Moreover, the TiO_2 rutile layer doesn't interact with other substances at room temperature. It neither reacts with oxygen, hydrogen sulfide, sulfur dioxide, ammonia and carbon dioxide, nor soluble in water, fatty acids and other organic acids and weak inorganic acid [32]-[34]. This behavior is beneficial in improving the corrosion resistance in simulated body fluid, and serves as an effective barrier layer, which physically separates the surface from the acids [23].

3.7. Water Contact Angle Measurements

The possibility of modifying and controlling the surface wettability of biological materials has attracted significant scientific and technological interest. Titanium and titanium alloys are widely used as biocompatible materials; therefore alterations of wetting behavior of these materials through modifying the surface properties (*i.e.* surface chemical composition, surface topography, and surface microstructure) are of great importance for the biomedical applications [35].

The wettability of untreated titanium and oxynitrided titanium are evaluated using contact angle technique which is based on Sessile Drop Method. Low contact angle means high wettability and high surface energy; high contact angle means low wettability and low surface energy [36]. **Figure 13** corresponds to the relation between the water contact angle and surface energy of the untreated and oxynitrided titanium as a function of plasma-processing power. One can observe from the figure that, the water contact angle of all surfaces is less than 90° , indicating the hydrophilic surface for all samples. The contact angle decreases from nearly 70° for the untreated titanium to reach a value of 42.6° for the sample that was oxynitrided at a plasma-processing power of 550 W, indicating the higher wettability for the oxynitrided titanium. The higher wettability and more hydrophilic surfaces are favorable for the adhesion, spread and proliferation of cells [37]. The increase in surface wettability is attributed to the change in the chemical composition and surface topography of the modified surface by forming oxynitrided phases. It is well known that during plasma surface modification, energetic atoms and

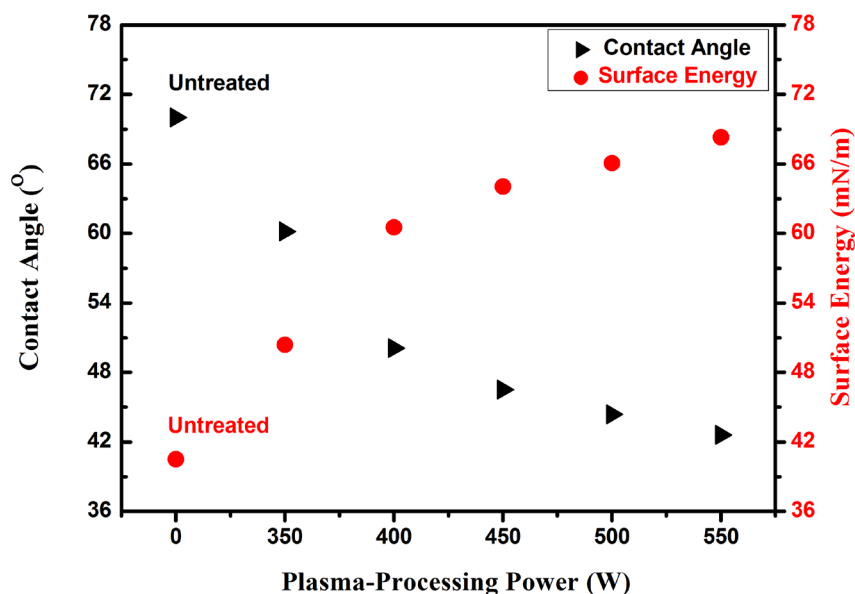


Figure 13. Water contact angle and surface energy of the untreated and oxynitrided titanium as a function of plasma-processing power.

other active plasma species react physically or chemically with the immersed metallic surface inside plasma and lead to plasma etching or cleaning process for the surface of the oxynitrided titanium. This in turn releases the organic contamination from the surface and consequently improves the surface wettability and hydrophilicity [38]. As observed in the same **Figure 13**, the surface energy of the oxynitrided titanium increases as the plasma-processing power increases to reach a value nearly 68 mN/m at a plasma-processing power of 550 W. The formation of hard phases of TiO₂ rutile, TiN_xO_y and Ti₂N increases the surface strengthening and consequently increases the surface energy.

4. Conclusion

The formation of oxynitrided phases TiO, TiO₂ rutile phase, TiN_xO_y and Ti₂N increases the microhardness of the oxynitrided layers up to 766 HV_{0.1} as the plasma processing power increases up to 550 W. Moreover, the values of wear and corrosion resistance for titanium oxynitride are improved compared to those for titanium. The friction coefficient decreases from nearly 0.75 for the titanium to nearly 0.3 for oxynitrided titanium. Furthermore, the oxynitrided layers revealed higher surface wettability and hydrophilicity compared to those of the untreated one. This combination between physical and electrochemical properties may provide the oxynitrided titanium with a better performance for different biomedical and industrial applications. One can conclude from these results that the RF plasma oxynitriding process can be considered as a powerful method for improving the physical and electrochemical properties of titanium.

Acknowledgements

The work was carried out as part of the research project of “Plasma Technology for Biomedical Applications”. This project was supported financially by the Science and Technology Development Fund (STDF), Egypt, Grant 3894.

References

- [1] Huang, P., Wang, F., Xu, K. and Han, Y. (2007) Mechanical Properties of Titania Prepared by Plasma Electrolytic Oxidation at Different Voltages. *Surface and Coatings Technology*, **201**, 5168-5171. <http://dx.doi.org/10.1016/j.surfcoat.2006.07.137>
- [2] Chen, F., Zhou, H., Chen, C. and Xia, Y.J. (2009) Study on the Tribological Performance of Ceramic Coatings on Titanium Alloy Surfaces Obtained through Microarc Oxidation. *Progress in Organic Coatings*, **64**, 264-267. <http://dx.doi.org/10.1016/j.porgcoat.2008.08.034>
- [3] Yerokhin, A.L., Niew, X., Leyland, A. and Matthews, A. (2000) Characterization of Oxide Films Produced by Plasma Electrolytic Oxidation of a Ti-6Al-4V Alloy. *Surface & Coating Technology*, **130**, 195-206. [http://dx.doi.org/10.1016/S0257-8972\(00\)00719-2](http://dx.doi.org/10.1016/S0257-8972(00)00719-2)
- [4] Wanga, Y., Jiang, B., Lei, T. and Guo, L. (2004) Dependence of Growth Features of Microarc Oxidation Coatings of Titanium Alloy on Control Modes of Alternate Pulse. *Materials Letters*, **58**, 1907-1911. <http://dx.doi.org/10.1016/j.matlet.2003.11.026>
- [5] Budinsky, K.G. (1991) Tribological Properties of Titanium Alloys. *Wear*, **151**, 203-217. [http://dx.doi.org/10.1016/0043-1648\(91\)90249-T](http://dx.doi.org/10.1016/0043-1648(91)90249-T)
- [6] Tsyganov, I.A., Maitz, M.F., Richter, E., Reuther, H. and Mashina, A.I. (2007) Hemocompatibility of Titanium-Based Coatings Prepared by Metal Plasma Immersion Ion Implantation and Deposition. *Nuclear Instruments and Methods in Physics Research Section B: Beam Interactions with Materials and Atoms*, **257**, 122-127. <http://dx.doi.org/10.1016/j.nimb.2006.12.169>
- [7] Vaz, F., Cerqueira, P., Rebouta, L., Nascimento, S.M.C., Alves, E., Goudeau, Ph. and Riviere, J.P. (2003) Preparation of Magnetron Sputtered TiN_xO_y Thin Films. *Surface and Coatings Technology*, **174-175**, 197-203. [http://dx.doi.org/10.1016/S0257-8972\(03\)00416-X](http://dx.doi.org/10.1016/S0257-8972(03)00416-X)
- [8] Venkataraj, S., Severin, D., Mohamed, S.H., Ngaruiya, J., Kappertz, O. and Wuttig, M. (2006) Towards Understanding the Superior Properties of Transition Metal Oxynitrides Prepared by Reactive DC Magnetron Sputtering. *Thin Solid Films*, **502**, 228-234. <http://dx.doi.org/10.1016/j.tsf.2005.07.280>
- [9] Bloyce, A., Morton, P. and Bell, T. (1994) ASM Handbook, Vol. 5. ASM International, Materials Park, OH, 835.
- [10] Minkevich, A.N. (1965) Thermo-Chemical Treatment of Metals and Alloys. Mashinostroene Press, Moscow, 325.
- [11] Goldschmidt, H.J. (1967) Interstitial Alloys. Butterworths, London. <http://dx.doi.org/10.1007/978-1-4899-5880-8>

- [12] El-Hossary, F., Negm, N.Z., Khalil, S.M. and Abd Elrahman, A.M. (2002) Formation and Properties of a Carbonitrided Layer in 304 Stainless Steel Using Different Radio Frequency Plasma Powers. *Thin Solid Film*, **405**, 179-185. [http://dx.doi.org/10.1016/S0040-6090\(01\)01729-1](http://dx.doi.org/10.1016/S0040-6090(01)01729-1)
- [13] El-Hossary, F.M., Negm, N.Z., Abd El-Rahman, A.M. and Hammad, M. (2009) Duplex Treatment of 304 AISI Stainless Steel Using RF Plasma Nitriding and Carbonitriding. *Materials Science and Engineering: C*, **29**, 1167-1173. <http://dx.doi.org/10.1016/j.msec.2008.09.049>
- [14] ASTM International (2011) ASTM Standard E384. West Conshohocken, PA, 19428-2959 USA.
- [15] Chappé, J.-M., Martin, N., Pierson, J.F., Terwagne, G., Lintymer, J., Gavaille, J. and Takadoum, J. (2004) Influence of Substrate Temperature on Titanium Oxynitride Thin Films Prepared by Reactive Sputtering. *Applied Surface Science*, **225**, 29-38. <http://dx.doi.org/10.1016/j.apsusc.2003.09.028>
- [16] Wang, Q., Zhang, P.-Z., Wei, D.-B., Wang, R.-N., Chen, X.-H. and Wang, H.-Y. (2013) Microstructure and Corrosion Resistance of Pure Titanium Surface Modified by Double-Glow Plasma Surface Alloying. *Material and Design*, **49**, 1042-1047. <http://dx.doi.org/10.1016/j.matdes.2013.02.054>
- [17] Rizzo, A., Signore, M.A., Mirengi, L. and Di Luccio, T. (2009) Synthesis and Characterization of Titanium and Zirconium Oxynitride Coatings. *Thin Solid Films*, **517**, 5956-5964.
- [18] Trenczek-Zajac, A., Radecka, M., Zakrzewska, K., Brudnik, A., Kusior, E., Bourgeois, S., Macro de Lucas, M.C. and Imhoff, L. (2009) Structural and Electrical Properties of Magnetron Sputtered Ti(ON) Thin Films: The Case of TiN Doped *in Situ* with Oxygen. *Journal of Power Sources*, **194**, 93-103. <http://dx.doi.org/10.1016/j.jpowsour.2008.12.112>
- [19] Graciani, J., Hamad, S. and Sanz, J.F. (2009) Changing the Physical and Chemical Properties of Titanium Oxynitrides $TiN_{1-x}O_x$ by Changing the Composition. *Physical Review B*, **80**, Article ID: 184112. <http://dx.doi.org/10.1103/PhysRevB.80.184112>
- [20] Tsyganove, I., Maitz, M.F. and Wieser, E. (2004) Blood Compatibility of Titanium-Based Coatings Prepared by Metal Plasma Immersion Ion Implantation and Deposition. *Applied Surface Science*, **235**, 156-163. <http://dx.doi.org/10.1016/j.apsusc.2004.05.134>
- [21] Williamson, G.K. and Hall, W.H. (1953) X-Ray Line Broadening from Filed Aluminium and Wolfram. *Acta Metallurgica*, **1**, 22-31. [http://dx.doi.org/10.1016/0001-6160\(53\)90006-6](http://dx.doi.org/10.1016/0001-6160(53)90006-6)
- [22] Scherrer, P. (1918) Bestimmung der Größe und der inneren Struktur von Kolloidteilchen mittels Röntgenstrahlen. *Nachrichten von der Gesellschaft Wissensch. zu Göttingen*, **26**, 98-100.
- [23] Wilson, A.J.C. (1943) The Reflexion of X-Rays from the "Anti-Phase Nuclei" of $AuCu_{3}$. *Proceedings of the Royal Society A: Mathematical, Physical and Engineering Sciences*, **181**, 360-368. <http://dx.doi.org/10.1098/rspa.1943.0013>
- [24] Navrotsky, A. and Kleppa, O.J. (2006) Enthalpy of the Anatase-Rutile Transformation. *Journal of the American Ceramic Society*, **50**, 626-626. <http://dx.doi.org/10.1111/j.1151-2916.1967.tb15013.x>
- [25] Abboud, J.H. (2013) Effect of Processing Parameters on Titanium Nitrided Surface Layers Produced by Laser Gas Nitriding. *Surface & Coatings Technology*, **214**, 19-29. <http://dx.doi.org/10.1016/j.surfcoat.2012.10.059>
- [26] Thomann, A.L., Basillais, A., Wegscheider, M., Boulmer-Leborgne, C., Pereira, A., Delaporte, P., Sentis, M. and Sauvage, T. (2004) Chemical and Structural Modifications of Laser Treated Iron Surfaces: Investigation of Laser Processing Parameters. *Applied Surface Science*, **230**, 350-363. <http://dx.doi.org/10.1016/j.apsusc.2004.02.060>
- [27] Yaskiv, O.I., Pohrel'yuk, I.M., Fedirko, V.M., Lee, D.B. and Tkachuk, O.V. (2011) Formation of Oxynitrides on Titanium Alloys by Gas Diffusion Treatment. *Thin Solid Films*, **519**, 6508-6514. <http://dx.doi.org/10.1016/j.tsf.2011.04.219>
- [28] Stratton, P. and Boodey, J. (2003) Case Hardening Titanium. *Proceedings of the 1st ASM International Surface Engineering and the 13th IFHTSE Congress*, ASM International, Materials Park, 22.
- [29] Kapczinski, M.P., Gil, C., Kinast, E.J. and Dos Santos, C.A. (2003) Surface Modification of Titanium by Plasma Nitriding. *Materials Research*, **6**, 265-271. <http://dx.doi.org/10.1590/S1516-14392003000200023>
- [30] Rautray, T.R., Narayanan, R. and Kim, K.-H. (2011) Ion Implantation of Titanium Based Biomaterials. *Progress in Materials Science*, **56**, 1137-1177. <http://dx.doi.org/10.1016/j.pmatsci.2011.03.002>
- [31] Pohrel'yuk, I.M., Fedirko, V.M., Tkachuk, O.V. and Proskurnyak, R.V. (2013) Corrosion Resistance of Ti-6Al-4V Alloy with Nitride Coatings in Ringer's Solution. *Corrosion Resistance*, **66**, 392-398.
- [32] Davis, J.R. (2000) Corrosion: Understanding the Basics. ASM International, Materials Park.
- [33] Basame, S.B. and White, H.S. (2000) Pitting Corrosion of Titanium the Relationship between Pitting Potential and Competitive Anion Adsorption at the Oxide Film/Electrolyte Interface. *Journal of the Electrochemical Society*, **147**, 1376-1381. <http://dx.doi.org/10.1149/1.1393364>
- [34] Habzaki, H., Shimizu, K., Skeldon, P., Thompson, G.E., Wood, G.C. and Zhou, X. (1997) Effects of Alloying Elements in Anodizing of Aluminium. *Transactions of the Institute of Metal Finishing*, **75**, 18.

- [35] Zeng, L., Liu, K., Zhang, Y.-C., Yue, X.-J., Song, G.-Q. and Ba, D.-C. (2009) The Microstructure and Wettability of the TiO_x Films Synthesized by Reactive DC Magnetron Sputtering. *Materials Science and Engineering: B*, **156**, 79-83. <http://dx.doi.org/10.1016/j.mseb.2008.11.043>
- [36] Kasemo, B. (2002) Biological Surface Science. *Surface Science*, **500**, 656-677. [http://dx.doi.org/10.1016/S0039-6028\(01\)01809-X](http://dx.doi.org/10.1016/S0039-6028(01)01809-X)
- [37] Baier, R.E., Shafrin, E.G. and Zisman, W.A. (1968) Adhesion: Mechanisms That Assist or Impede It. *Science*, **162**, 1360-1368. <http://dx.doi.org/10.1126/science.162.3860.1360>
- [38] Yin, H.Y., Jin, Z.S., Zhang, S.L., Wang, S.B. and Zhang, Z.J. (2002) Reason for the Loss of Hydrophilicity of TiO₂ Film and Its Photocatalytic Regeneration. *Science in China Series B: Chemistry*, **45**, 625-632.

Scientific Research Publishing (SCIRP) is one of the largest Open Access journal publishers. It is currently publishing more than 200 open access, online, peer-reviewed journals covering a wide range of academic disciplines. SCIRP serves the worldwide academic communities and contributes to the progress and application of science with its publication.

Other selected journals from SCIRP are listed as below. Submit your manuscript to us via either submit@scirp.org or [Online Submission Portal](#).

